

# SIMULATION OF MINI-BAND FORMATION IN TRIPLE SI QUANTUM WELLS BASED RESONANT TUNNELING DIODE

Sri Purwiyanti<sup>a,b</sup>, Ratno Nuryadi<sup>c</sup>, Djoko Hartanto<sup>b</sup>

<sup>a</sup>Faculty of Engineering

University of Lampung, Bandar Lampung, Indonesia

E-mail : sripurwiyantisurya@yahoo.com

<sup>b</sup>Faculty of Engineering

University of Indonesia, Depok 16424, Indonesia

E-mail : djoko@ee.ui.ac.id.

<sup>c</sup>Center for Material Technology

Agency for Assessment And Application of Technology (BPPT),

M.H. Thamrin Street No. 8, 10340, Jakarta, Indonesia

E-mail : ratnon@gmail.com

**Abstract---** In this work, we investigate the formation of mini-band energy in triple Si quantum wells-based resonance tunnelling diode focusing on the effect of applied bias on the band. The formation of mini-bands is obtained from the calculation of electron tunnelling probability through the wells. The calculation is done based on transfer matrix method. The simulation results show the mini-band formation due to the appearance of discrete energy group. The changes of applied bias, quantum well width and barrier thickness causes the change of the mini-band width. These results indicate that the device structure and applied bias condition play a key role on the formation of mini-band energy in the quantum wells.

**Keywords---** Triple quantum wells, mini-band discrete energy, applied bias, tunnelling probability

## 1. INTRODUCTION

Recent modern fabrication technology allows us for the fabrication of nanometer-scaled quantum wells, which is possible to observe resonance tunnelling phenomena. One important parameter in the design of quantum wells is to find out the position of energy levels inside the wells when the electric field is given or not [1]. These levels enhance high transmission probability of electron due to wave interference effect. A solution of Schrodinger equation in single quantum well forms discrete energy levels, while the solution in the multiple quantum wells produces energy mini-bands (sub-bands) as well as those for the superlattice structure. The main difference between mini-bands in the multiple wells and ones in the superlattice is a presence (or not) of discrete energy levels inside the mini-bands. In the superlattice, the energy levels are almost continuously formed in the mini-bands, while, in N numbers of wells, N number of very closed distance discrete energy levels are formed inside the mini-bands. For instance, two couple quantum wells result in two discrete energy levels in mini-bands, and the three wells results in three energy levels in the bands.

So far, resonant tunneling devices (RTDs) consisting of single and double wells have been reported both in experimental and simulation [2]-[6]. However, RTD having triple quantum wells or more has not been understood well. Particularly, the presence of discrete energy levels inside mini-band is needed to be clarified. In this work, we investigate the formation of mini-bands in triple quantum wells based RTD focusing on the effect of applied bias on the bands. Here, the device is made from the combination of Si/SiO<sub>2</sub> materials having 4-potential barriers and 3-quantum wells. The formation of mini-bands is obtained from the calculation of electron tunnelling probability through the wells.

## 2. DEVICE STRUCTURE AND SIMULATION METHOD

The structure which forms triple quantum wells is schematically shown in Fig.1. The structure consists of two heavily doped n<sup>+</sup> Si layers in the edges (right and left), four SiO<sub>2</sub> layers and the three low-doped Si layers regions. The conduction band energy for this structure is shown in Fig. 2. Consider the electron affinity of Si is 4.05 eV, and that of SiO<sub>2</sub> is 0.9 eV, it is obtained that the potential barrier height is 3.15 eV. As a result, the three quantum wells are formed in the silicon layers. Here, the width of Si and SiO<sub>2</sub> layers is designed to be 10 nm and 5 nm, respectively.

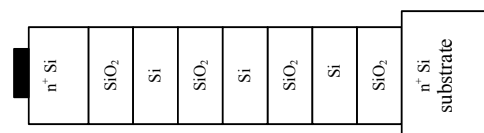


Fig. 1 The structure of 3 triple quantum wells

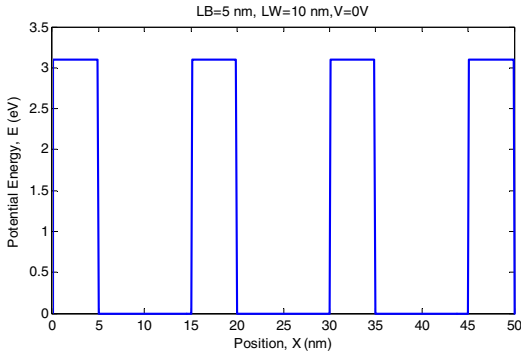


Fig. 2 The conduction band energy diagram.

We use calculation of electron tunnelling probability in the conduction band in order to determine the energy levels forming the mini-bands. Here, Schrodinger equation in triple quantum wells is directly solved based on transfer matrix method [7]-[10]. Such method is usually used to calculate the tunnelling probability in Resonance Tunnelling Diode (RTD) structure. By this method, the resonance tunnelling phenomena which is induced by the interference of electron wave, can be appeared. The transfer matrix method is mainly explained using Fig.2 as follows.

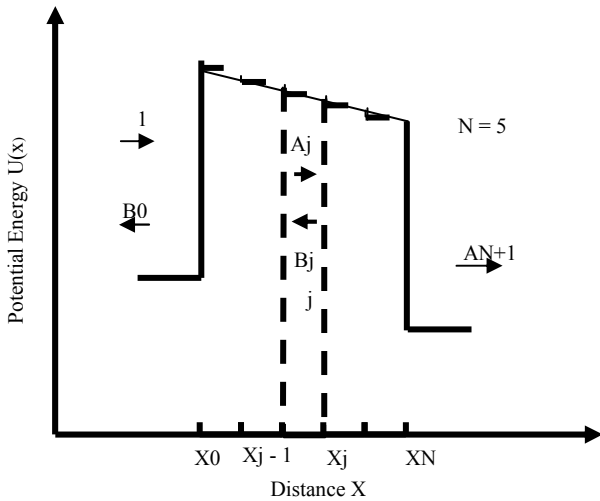


Fig. 3 Energy band diagram of 3 triple quantum wells

Consider the Fig. 3, electron wave function  $\psi_j$  in the point  $j$  moving in  $x$  direction can be expressed by

$$\psi_j(x) = A_j \exp(ik_j x) + B_j \exp(-ik_j x) \quad (1)$$

where

$$k_j = \sqrt{2m_j^*(E - U_j)/\hbar}$$

Here  $U_j$  is the potential energy barrier,  $E$  is the electron energy,  $m_j^*$  is the effective mass, and  $\hbar$  is the reduce Planck's constant.

Consider the continuity of  $\psi_j$  and  $(1/m_j^*) (d\psi_j/dx)$  at each boundary of Si/SiO<sub>2</sub>,  $A_j$  and  $B_j$  in eq. (1) can be calculated from the following equation

$$\begin{pmatrix} A_j \\ B_j \end{pmatrix} = \prod_{i=0}^{j-1} M_i \begin{pmatrix} A_0 \\ B_0 \end{pmatrix} \quad (2)$$

where

$$M_i = \frac{1}{2} \begin{bmatrix} (1+S_i)\exp[-i(k_{i+1}-k_i)x_i] & (1-S_i)\exp[-i(k_{i+1}+k_i)x_i] \\ (1-S_i)\exp[i(k_{i-1}+k_i)x_i] & (1+S_i)\exp[i(k_{i-1}-k_i)x_i] \end{bmatrix} \quad (3)$$

and

$$S_i = \frac{m_{i+1}^* k_i}{m_i^* k_{i+1}}$$

It can be seen in eq. (3) that  $M_i$  is  $2 \times 2$  matrices and  $N+1$  of  $M$  matrix is needed in order to obtain the values of  $A$  and  $B$  in the position of point  $N$  (see Fig. 3). Here,  $N$  is the total number of grid. By assuming that the amplitude  $A_0=1$  and  $B_{N+1}=0$  (no reflection in point  $N+1$ ) in Eq. (2) for  $j=N+1$ , the transmission amplitude  $A_{N+1}$  and the transmission probability  $T(E)$  can be calculated as follows:

$$A_{N+1} = \frac{m_{N+1}^* k_0}{m_0^* k_{N+1}} \frac{1}{M_{22}} \quad (4)$$

$$T(E) = \frac{m_0^* k_{N+1}}{m_{N+1}^* k_0} |A_{N+1}|^2 \quad (5)$$

where  $M = \begin{bmatrix} M_{11} & M_{12} \\ M_{21} & M_{22} \end{bmatrix} = \prod_{i=0}^N M_i$

### 3. RESULTS AND DISCUSSION

The simulation program is executed on the various applied voltage ( $V_{app}$ ), barrier thickness ( $LB$ ), and quantum well thickness ( $Lw$ ). Here, we use the Si and SiO<sub>2</sub> effective masses of 0.26 and 0.7, respectively. Fig. 4 shows the energy band diagram (a) and calculated tunnelling probability (b) obtained from the device with barrier width of 4 nm, well width of 10 nm, and applied voltage of 0.2 V. The tunnelling probability is investigated for the range of discrete energy from 0 to 2.48 eV. This limited energy is applied because the presence of unusual phenomenon, which is will be explain in the next paper.

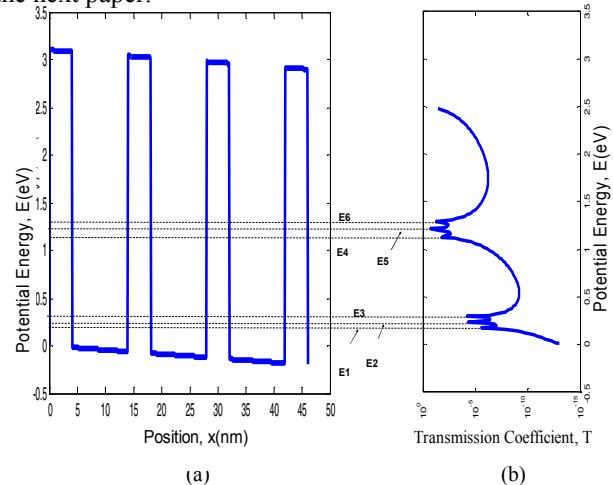


Fig.4 The mini-band formation on 4-barrier Si/SiO<sub>2</sub> structure with  $V_{app} = 0.2V$ ,  $LB = 4$  nm, and  $LW = 10$  nm.

It can be seen that the tunnelling probability has two big peaks, i.e. peak at around 0.2 eV and one at around 1.3 eV. The most important result here is that each peak has three small peaks, i.e., peaks E1, E2 and E3 on lower big peaks and peaks E4, E5 and E6 on the bigger one. Such peaks may be caused by interference of electron wave in three quantum wells. Therefore, each small peak (E1-E6) is attributed to generated-energy level, as shown in Fig. 4(a). The lower and bigger groups of energy levels like mini-band as well as one formed superlattice structure.

#### A. Influence of Applied Voltage on Mini-band Energy.

Fig. 5 shows the transmission probability vs energy graph with different applied bias. The potential barrier is rectangular with barrier width (LB) = 5 nm, and quantum well width (LW) = 10 nm. The applied bias with  $V_{app} = 0$  V develops two big-peaks and each of peak splits to three small peak. It is noted that the split in lower energy peak is shown in insert figure (Fig. 5(a)). It is also found that for  $V_{app} = 0.5$  V (fig. 5(b)), there are three big peaks (mini-bands) that also split to small peak discrete energies.

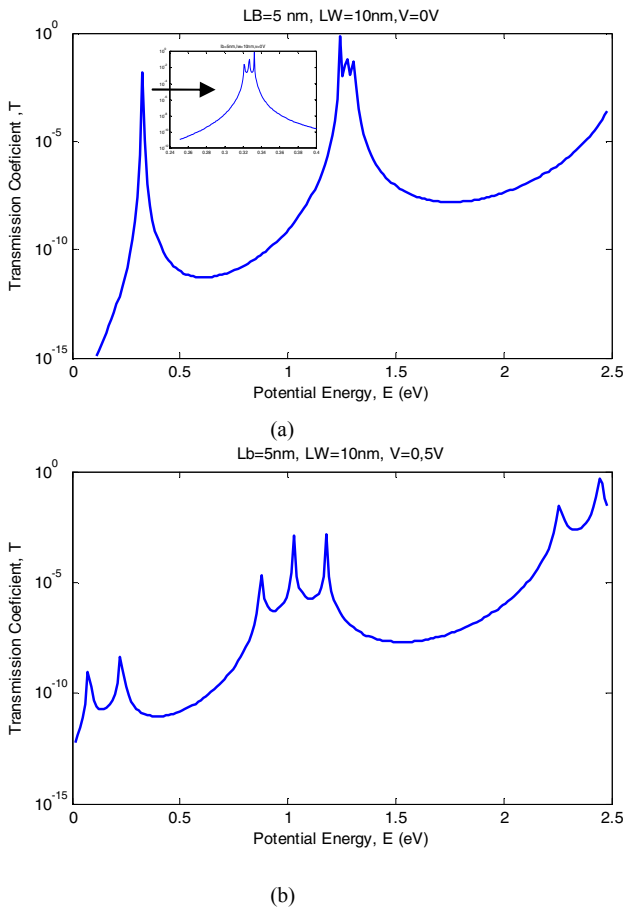


Fig.5 The influence of applied bias on mini-band energy at (a)  $V_{app} = 0$  V and (b)  $V_{app} = 1$  V.

The comparison of graph in fig.5 (a) and (b) indicates that the mini-band in fig 5(b) is wider than that in Fig. 5(a). That is caused by the increase of the applied voltage which decreases the potential barrier. The decrease in potential barrier also increase the transmission probability as shown in Fig. 5.

Fig. 6 presents the change of small peaks, which represent discrete energy levels, when the applied bias is varied from 0 to 10 V. The interesting phenomenon is clearly found in the second mini-band. In this mini-band, the width is around 0.02 eV for  $V_{app} = 0$  V and the one is around 0.6 eV for a larger value of applied bias ( $V_{app} = 1$  V). It indicates that the increase in applied bias causes the increase in mini-bands width.

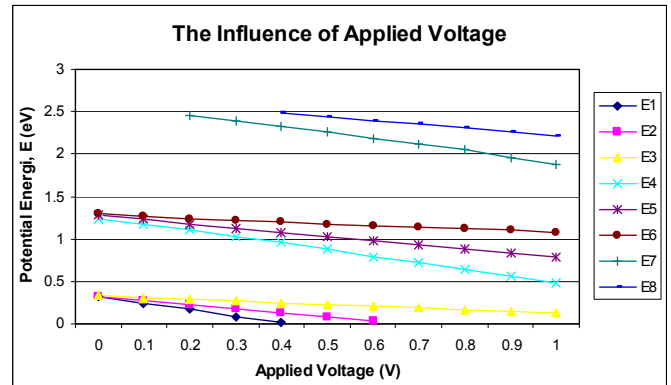


Fig. 6 The change of peak discrete energy value caused the applied bias. The bias is applied from 0 – 1 V, with  $LB = 5$  nm and  $LW = 10$  nm.

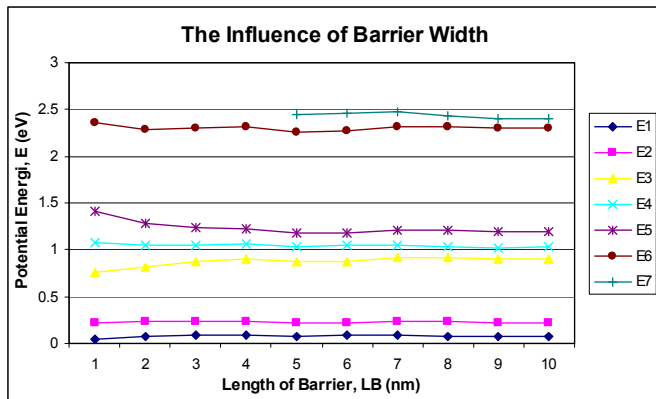
It is also found that the increase in applied bias causes the decrease in discrete energy peak. This can be clearly seen in line E4, where the peak energies of 1.242 eV, 0.8804 eV and 0.4836 eV are found for  $V_{app} = 0$  V, 0.5 V and 1 V, respectively.

#### B. Influence of potential barrier and well width

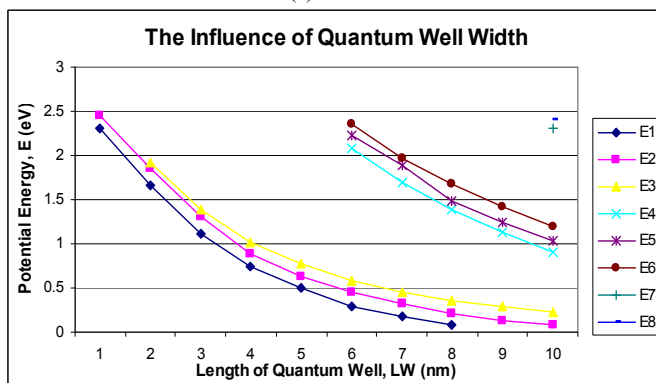
The influence of barrier thickness on the mini-band energy is shown in Fig. 7 (a), where the parameter  $LW$  is 10 nm and  $V_{app}$  is 0.5 V. We choose the second mini-band energy as sample in order to explain the characteristics. As we can see that the width of the mini band (E5-E3) decrease from 0.8 eV for  $LB = 1$  nm to about 0.3 eV for  $LB = 10$  nm. This indicates that the increase in barrier thickness causes the increase in mini-band width.

The influence of the quantum well width on the mini-band energy is shown in Fig. 7 (b), where the parameter  $LB$  is 10 nm and  $V_{app}$  is 0.5 V. The graph shows the decrease of discrete energy levels due to the increase in well width. It can be seen that all discrete energies show the same behaviour. The discrete energy levels decrease with the increasing the quantum well width. For example, let's consider the line E2. The energy level is found to be 2.5 eV for  $LW = 1$  nm and 0.1 eV for  $LW = 10$  nm. Figure 7 (b) also indicates the increase of mini-band width with increasing the quantum well width. This

phenomenon can be clearly seen in the second mini band. Here, the width increases from 0.2 eV for LW=1 nm to 0.45 eV for LW = 8 nm.



(a)



(b)

Fig.7 (a) The influence of barrier width to mini-band width with  $V_{app} = 0.5V$  and LW is 10 nm. (b) The influence of the quantum well width to mini-band energy with  $V_{app} = 0.5V$  and LB is 10 nm.

#### 4. CONCLUSIONS

We studied the effect of applied bias, the barrier width, and the quantum well width on the mini-band energy in three Si quantum wells system. The calculation was done based on transfer matrix method. The simulation results show the mini-band formation due to the appearance of discrete energy group. The increase of applied bias and quantum well width causes the increase of mini-band width but the decrease of the discrete energy peak. We also found that the mini-band width depends on the applied bias and the device structure. Therefore, the control of voltage bias, barrier thickness and quantum well width is required in order to realize good performance of the multiple quantum wells structure.

#### REFERENCES

[1] G. W. Hanson, "Fundamentals of Nanoelectronics", Pearson Prentice Hall, New Jersey, 2008.  
 [2] C.E. Simion and C.I. Ciucu, "Triple-barrier resonant tunnelling: A Transfer matrix Approach," *Romanian Reports in Physics*, vol. 59, No. 3, pp.805-817, 2007.

[3] K. M. S. V. Bandara, J. W. Choe, and M. H. Francombe, "GaAs/AlGaAs Superlattice Miniband Detector with 14.5  $\mu\text{m}$  peak response", *Appl. Phys. Lett.* 60 (24), 15 June 1992.  
 [4] R. Djelti, S. Bentata, and Z. Aziz, "Electronic states nature of trimer height barrier disorder superlattices," *Journal of Applied Sciences* 7 (3): 417-420, 2007.  
 [5] D. Vashaee, Yan Zhang, A. Shakouri, G. Zeng, and Yi Jen Chiu, "Cross-plane Seebeck Coefficient in Superlattice Structure in The Miniband Conduction Regime", *Physical Review B* 74, 195315, 2006.  
 [6] K. D. Choquette, D. K. Misemer and L. McCaughan, "Electronic Structure of Short-Period n-p GaAs Doping Superlattices", *Physical review B*, Volume 43, Number 9, March 1991.  
 [7] A. Zarifkar and A. M. Bagherabadi, "Numerical analysis of triple-barrier GaAs/Al<sub>x</sub>Ga<sub>1-x</sub>As Resonant tunnelling structure using PMM approach," *IJCSNS*, vol. 8, no. 6, June 2008.  
 [8] R. Nuryadi, "The simulation of tunnelling probability calculation on Resonant Tunneling Diode (RTD)," *SNIKA 200*, ISSN 1907-882X, 2009.  
 [9] R. Nuryadi, "The tunnelling probability calculation on nanometer potential barrier". Paper.  
 [10] Y. Ando and T. Itoh, "Calculation of transmission tunneling current across arbitrary potential barriers", *J. Appl. Phys.*, 61(4):1497-1502, 1987.